FORGE

Fate Of Repository Gases

European Commission FP7

Mont Terri
HG-C Experiment
GP-A and GS Experiments

FORGE Report D5.15

	Name	Organisation	Signature	Date
Compiled	MARIA TERESA ZANDARIN	UPC		June 2013
Verified	RP Shaw	BGS		14th October 2013
Approved	RP Shaw	BGS		14th October 2013

Keywords.

Mont Terri URL; HG-C test; GPA/GS experiments; Opalinus Clay; Gas flow; modelling

Bibliographical reference

MARIA TERESA ZANDARIN, SEBASTIAN OLIVELLA AND EDUARDO ALONSO. 2013. Mont Terri HG-C Experiment GP-A and GS Experiments

FORGE Report D5.15. 16pp.

Euratom 7th Framework Programme Project: FORGE

EURATOM

Fate of repository gases (FORGE)

The multiple barrier concept is the cornerstone of all proposed schemes for underground disposal of radioactive wastes. The concept invokes a series of barriers, both engineered and natural, between the waste and the surface. Achieving this concept is the primary objective of all disposal programmes, from site appraisal and characterisation to repository design and construction. However, the performance of the repository as a whole (waste, buffer, engineering disturbed zone, host rock), and in particular its gas transport properties, are still poorly understood. Issues still to be adequately examined that relate to understanding basic processes include: dilational versus visco-capillary flow mechanisms; long-term integrity of seals, in particular gas flow along contacts; role of the EDZ as a conduit for preferential flow; laboratory to field up-scaling. Understanding gas generation and migration is thus vital in the quantitative assessment of repositories and is the focus of the research in this integrated, multi-disciplinary project. The FORGE project is a pan-European project with links to international radioactive waste management organisations, regulators and academia, specifically designed to tackle the key research issues associated with the generation and movement of repository gasses. Of particular importance are the long-term performance of bentonite buffers, plastic clays, indurated mudrocks and crystalline formations. Further experimental data are required to reduce uncertainty relating to the quantitative treatment of gas in performance assessment. FORGE will address these issues through a series of laboratory and field-scale experiments, including the development of new methods for up-scaling allowing the optimisation of concepts through detailed scenario analysis. The FORGE partners are committed to training and CPD through a broad portfolio of training opportunities and initiatives which form a significant part of the project.

Further details on the FORGE project and its outcomes can be accessed at www.FORGEproject.org.

Contact details:

MARIA TERESA ZANDARIN, SEBASTIAN OLIVELLA AND EDUARDO ALONSO

Department of Geotechnical Engineering and Geosciences

Universitat Politècnica de Catalunya

Jordi Girona 1-3

08034 Barcelona

Spain

Departament d'Enginyeria
del Terreny, Cartogràfica i Geofísica
UNIVERSITAT POLITÈCNICA DE CATALUNYA

Mont Terri

HG-C Experiement

GP-A and GS Experiments

DELIVERABLE

Maria Teresa Zandarin

Sebastian Olivella

Eduardo Alonso

Contents

INTRODUCTION 3

Description of the test geometry 4

Geometry and materials used in the model 5

Constitutive law of materials and parameters 6

Comparison between numerical and experimental results 9

Conclusions 16

References 16

INTRODUCTION

The present report synthesizes the results of the numerical simulation of the experiments GP-A/GS. The experiments were carried out to study the two-phase flow properties of the Opalinus clay at Mont Terri. The test includes two parts; the first part of the program was the determination of the frac and reopening pressures characterization of the formation subsequent to the hydro-frac. The second part consisted in a re-hydration phase, the water and gas tests were repeated in order to characterize the fracture self sealing behaviour in the Opalinus clay (Enachescu et al., 2002). The numerical simulation is focus in the second part of the test. In Table 1 are indicated the phases of the test and in blue are remarked the phases simulated.

Table 1 Phases of the test. In blue are remarked the phases simulated.

Phase Name	Elapsed Hours		Test Phase	Test event
	Start	End		
Hyd1PRE	1	460	Hydro 1	Pretest
Hyd1PI1	460	478	Hydro 1	Pulse Test 1
Hyd1HI1	478	486	Hydro 1	Constant Head Test (1020 kPa)
Hyd1HIS1	486	503	Hydro 1	Shut-in
Hyd1HI2	503	511	Hydro 1	Constant Head Test (2070 kPa)
Hyd1HIS2	511	1631	Hydro 1	Shut-in
Gas1PI1	1631	2283	Gas 1	Gas Pulse Step 1 (1190 kPa)
Gas1PI2	2283	2355	Gas 1	Gas Pulse Step 2 (1280 kPa)
Gas1PI3	2355	2451	Gas 1	Gas Pulse Step 3 (1920 kPa)
Gas1PI4	2451	2879	Gas 1	Gas Pulse Step 4 (2780 kPa)
Gas1REL	2879	3311	Gas 1	Recovery
FracPre	3336	3338	Frac	Step pressure increase
Frac1	3338	3339	Frac	Second frac cycle -
Frac2	3339	3341	Frac	Refrac Cycle 1
Frac3	3341	3358	Frac	Refrac Cycle 2
Hyd2PI1	3359	3365	Hydro 2	Pulse Test 1 (1835 kPa)
Hyd2PI2	3365	3366	Hydro 2	Pulse Test 2 (2005 kPa)
Hyd2PI3	3366	3367	Hydro 2	Pulse Test 3 (3604 kPa)
Hyd2PI4	3367	3369	Hydro 2	Pulse Test 4 (4548 kPa)
Hyd2HI	3369	3370	Hydro 2	Constant head injection (6682 kPa)
Hyd2HIS	3370	3381	Hydro 2	Shut-in
Gas2PI	3383	4964	Gas 2	Gas pulse Nitrogen Injection
Gas3PRE	5020	5038	Gas 3	Pretest
Gas3GRI	5038	5054	Gas 3	Gas constant rate nitrogen injection (0.1 mln/min)
Gas3GRIS	5054	8689	Gas 3	Shut-in
Hyd3HI1	8689	9414	Hydro 3	Constant head water injection 1 (1845 kPa)
Hyd3HI2	9414	10852	Hydro 3	Constant head water injection 2 (2380 kPa)
Hyd3HIS2	10852	13870	Hydro 3	Shut-in
Gas4GRI	13870	13962	Gas 4	Gas constant rate nitrogen injection (20.3 mln/min
Gas4GRIS	13962	20940	Gas 4	Shut-in

Description of the test geometry

Four boreholes were drilled parallel, and perpendicular on the Opalinus clay bedding planes. The borehole diameter was 101mm. At borehole BGS2 was injected the water and the gas according to the test phase and at borehole BGS1 were measured the pressure transmitted through the bedding plane. The distance between BGS2 and BGS1 was 1.4 m. The displacements were measured at boreholes BGS3 and BGS4 using extensometer located at different depth. The distance between boreholes BGS2, BGS3 and BGS4 was 0.7m respectively (Figs. 1a and 1 b) (Enachescu et al., 2002).

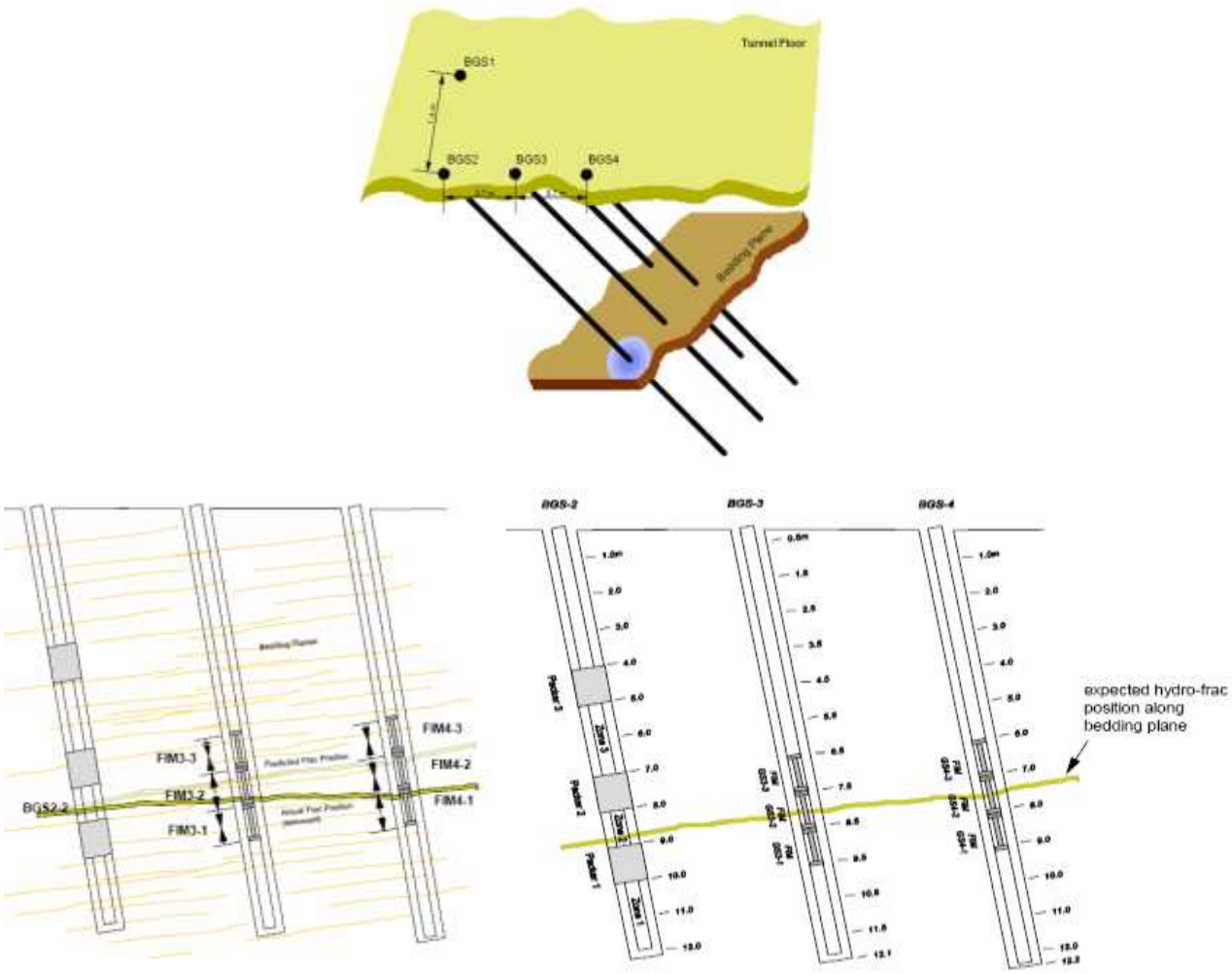

Figure 1 a: Schematic view of borehole location and bedding plane. 1b: Schematic view of boreholes BGS2, BGS3 and BGS4 including the position of the extensometers.

Geometry and materials used in the model

The geometry used in the simulation is axi-symmetric and it has 15m of length and 15m of depth (Fig. 2a). Four materials were considered in the model, the Opalinus clay, the Fracture and Water in the borehole BGS2 and Water 1 in borehole BGS1 (Fig 2 b).

The Fracture is located at a depth equal to 8.50m, according to the frac position shown in Figure 1b.

The porosity of Water 1 was calculated considered the real volume of BGS1. The Opalinus clay, Water and Water 1 were discretized using 556 continuum elements, whereas, the Fracture was discretized using 19 joint elements. The constitutive laws and parameters of the materials are summarized in next section.

The initial conditions are summarized in Table 2. All the materials are considered saturated with a liquid pressure P_l = 1.4MPa. And the injection of liquid or gas it was imposed at the upper boundary of BGS2 indicated in Figure 2 b.

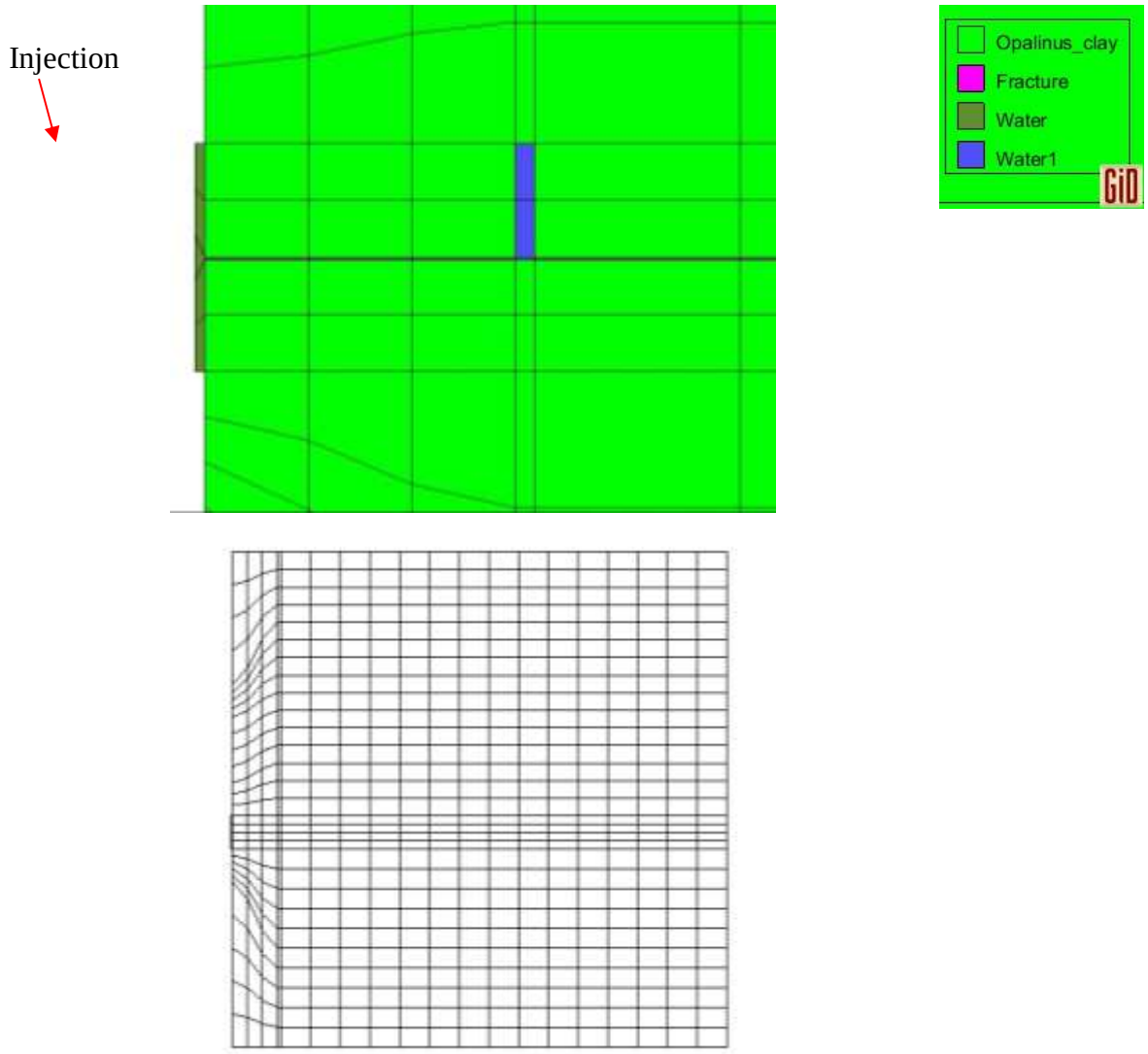

Figure 2 a: geometry of the model and finite element mesh. 2 b: Materials used in the model.

Constitutive law of materials and parameters

For the Opalinus clay, Water and Water 1 a linear elastic law was considered for model their mechanical behaviour and a constant intrinsic permeability for the hydraulic model. The water retention curve adopted for the Opalinus clay is the curve proposed by Sanchez, (2008). And for Water and Water 1 was adopted the Van Genutchen´s curve, (1980).

However for the Fracture it was considered the joint element with a non-linear elastic law. This law calculated the normal stiffness considering the changing of the joint aperture as Equation 2:

$$\begin{Bmatrix} \sigma' \\ \tau \end{Bmatrix} = \begin{bmatrix} K_n & 0 \\ 0 & K_s \end{bmatrix} \begin{Bmatrix} u_n \\ u_s \end{Bmatrix} \qquad 1$$

$$K_n = \frac{m}{\mathrm{a} - \mathrm{a}_{\min}} \qquad 2$$

where σ' is normal net stress, τ is the tangential stresses, u_n and u_s are the normal tangential displacement of the joint element, K_n and K_s are the normal and tangential stiffness respectively, *m* is a parameter of the model; a is the opening of the element, and a_{min} is the minimum opening of the element (at this opening the element is closed).

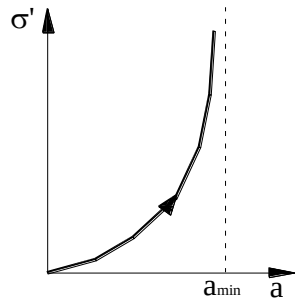

Figure 3: Elastic constitutive law of the joint element. Normal stiffness depends on joint opening.

The longitudinal fluid flow through the Fracture is considered laminar. Based on this hypothesis, the hydraulic conductivity of the joint is calculated by the following cubic law:

$$K_l = \frac{\rho g}{\mu} \frac{e^3}{12} \qquad 3$$

where r is the fluid density; g is the gravity, and m is the fluid viscosity and e is the hydraulic permeability.

Therefore the equation of intrinsic permeability is:

$$k_l = \frac{e^2}{12} \qquad 4$$

In this case the hydraulic opening (e) of the Fracture is calculated adding to the initial hydraulic opening (calculated by Barton (1985)'s law) the increase or decrease of the Fracture opening calculated by the elastic law in each time period:

$$e = \frac{\mathrm{a}^2}{JRC^{2.5}} + \Delta\mathrm{a} \qquad 5$$

The transversal intrinsic permeability k_t is considered to be equal to the continuum media.

The degree of saturation of joints is calculated using the standard retention curve of van Genuchten (van Genuchten, 1980):

$$S_l = \left[1 + \left(\frac{\Psi}{P}\right)^{\frac{1}{1-\lambda}}\right]^{-\lambda} \qquad 6$$

where S_l is the liquid degree of saturation; $\Psi = P_g - P_l$ is the current suction; λ is a model parameter, and P is the air entry pressure necessary to desaturate joints.

The variation in the joint opening also causes changes in air entry pressure (Olivella & Alonso, 2008). The air entry pressure necessary to desaturate the joint depends on its hydraulic opening, that is:

$$P_0 = \sigma\left(\frac{1}{r_1} + \frac{1}{r_2}\right) = \frac{2\sigma}{e} \qquad 7$$

which is obtained when $(1/r_1) = 0$ and $r_2 = e/2$. In this case the wetting angle was assumed to equal zero. If Equation 8 is combined by means Equation 5, the capillary pressure necessary to start desaturation is obtained as:

$$P = P_0 \frac{\sqrt{k_{l0}}}{\sqrt{k_l}} \qquad 8$$

And the relative permeability of the materials is adopted as:

$$k_{rl} = k_{rg} = S^3 \qquad 9$$

The parameters of the materials are summarized in Table 2.

Table 2: Initial conditions and parameters of the materials.

Material	Initial conditions				Hydraulic properties						Mechanical properties
	n_0	ρd [kg/m3]	Sr [%]	P_{l0}. [MPa]	kx [m2]	ky [m2]	P0 [MPa]	λ	Pd [MPa]	λd	Elastic parameter
Opalinus Clay	0.137	2170	100	1.4	9.0×10^{-21}	1.1×10^{-21}	8	0.2	700	2.38	E [MPa]=4×10^3 υ=0.27
Joint	**-**	**-**	**100**	**1.4**	**Dependant with the aperture**	**1.0×10^{-16}**	**1**	**0.3**	**-**	**-**	**m[MPa] =1.0×10^8 Kt[MPa/m]=1.0×10^6 a0 [m]=0.01**
BGS2Z2 (Water)	0.99	-	100	1.4	1.0×10^{-12}	1.0×10^{-12}	1×10^{-4}	0.6	-	-	E [MPa]=1.0 υ=0.49
BGS1Z2 (Water 1)	0.015	-	100	1.4	1.0×10^{-12}	1.0×10^{-12}	1×10^{-4}	0.6	-	-	E [MPa]=1.0 υ=0.49

Comparison between numerical and experimental results

In this section it is shown a comparison between numerical and experimental data (Enachescu et al., 2002) obtained for each phase. In Table 1 it is shown that water pressure used in phases Hydro 2 and Hydro 3 and the gas injection rate used in phases Gas 3 and Gas 4 are well reported. However the gas injection rate used in phase Gas 2 are not recorded then for the simulation a gas flow equal to 1.0×10^{-5} kg/s was adopted.

The displacements measured by the extensometers were compared with the displacement calculated by differentiation between the displacement obtained from the model at depth 6.5, 7.5, 8.5 and 9.5m for the borehole BGS3 and at depth 6, 7, 8 and 9m for borehole BGS4.

In general it is observed that pressures are reproduced well, however the displacement are qualitatively capture. Specially, the displacements calculated for the phase Gas 2 presented a great difference with the measured displacements (Figs 9 and 10). This could be a consequence of adopted a greater injection rate than used it.

Also, a contour plot of pressure is drawn for each phase. In these plots it is observed that the Fracture is a preferential path of flows due to its great transmissivity.

In Figure 24 it is drawn the evolution of the degree of saturation of the Fracture at different distance from the injection borehole (BGS2) during the tests. It is observed that the Fracture desaturate during gas injection phases and it hydrate during water injection. And these phenomena are more evident for the length of the Fracture next to the borehole.

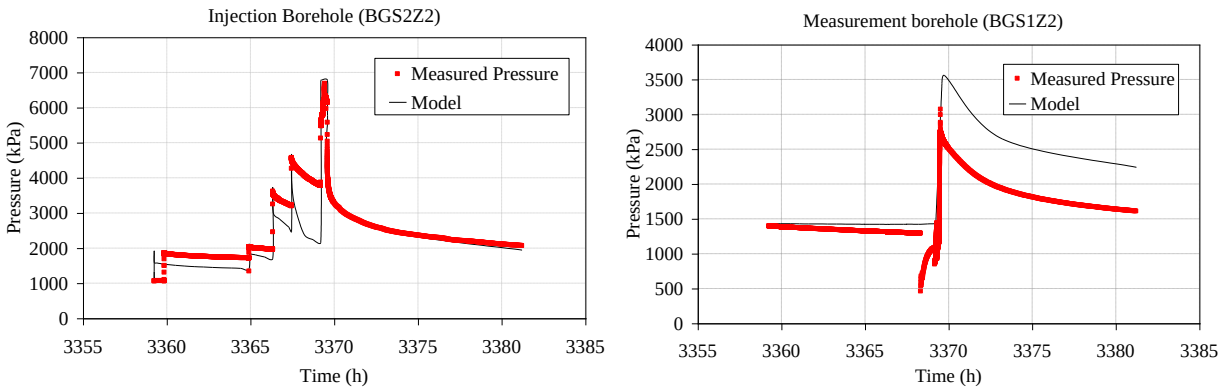

Figure 4: Comparison between numerical and experimental pressures at injection borehole BGS2 and at measurement borehole BGS1 for phase “Hydro2”

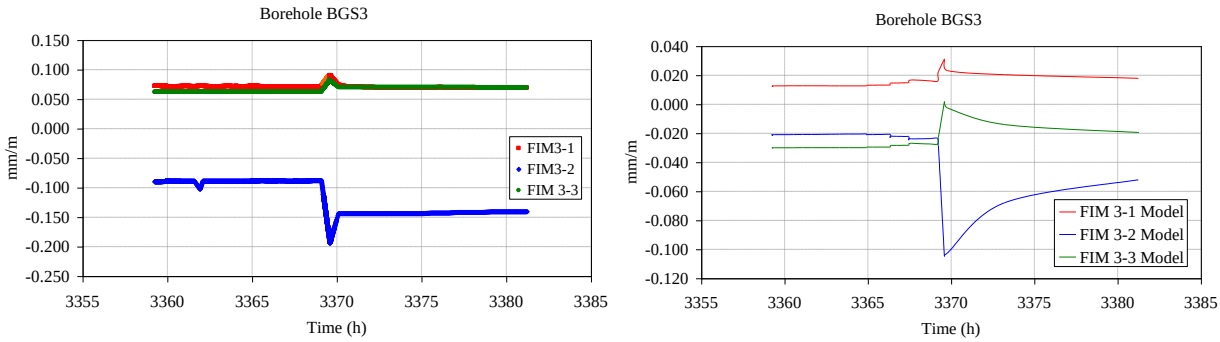

Figure 5: Displacement measured at BGS3 (left) and displacement calculated (right) for phase "Hydro2"

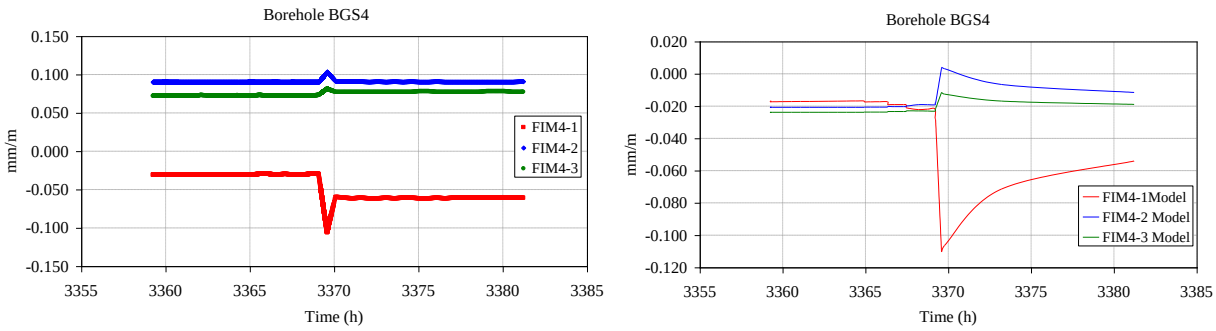

Figure 6: Displacement measured at BGS4 (left) and displacement calculated (right) for phase "Hydro2"

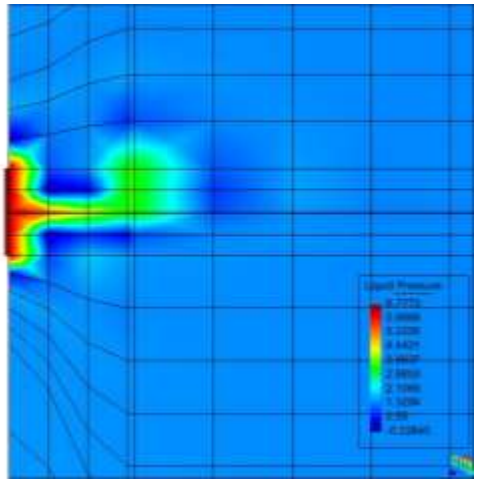

Figure 7: Contour plot of liquid pressure at time 3380 hours

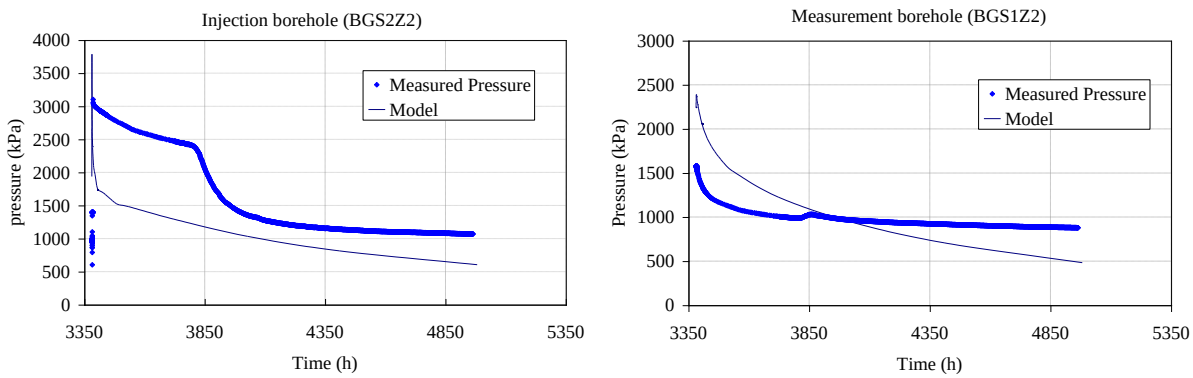

Figure 8: Comparison between numerical and experimental pressures at injection borehole BGS2 and at measurement borehole BGS1 for phase "Gas 2"

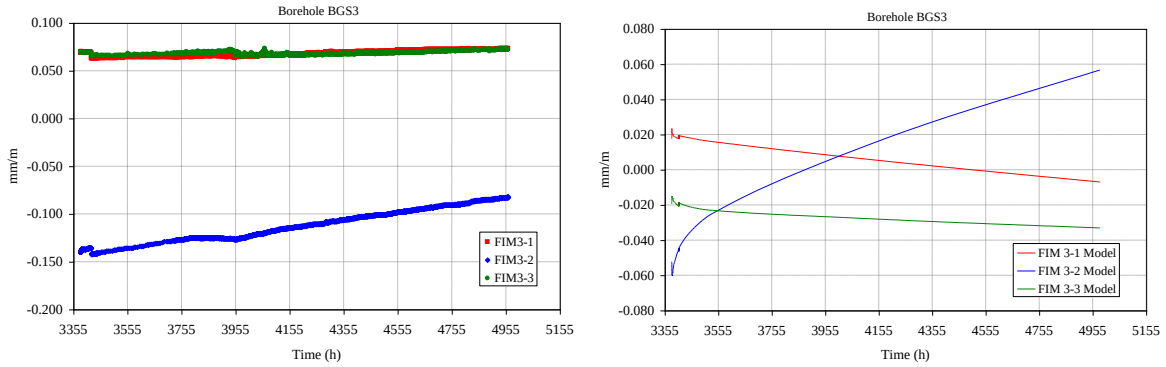

Figure 9: Displacement measured at BGS3 (left) and calculated (right) for phase "Gas2"

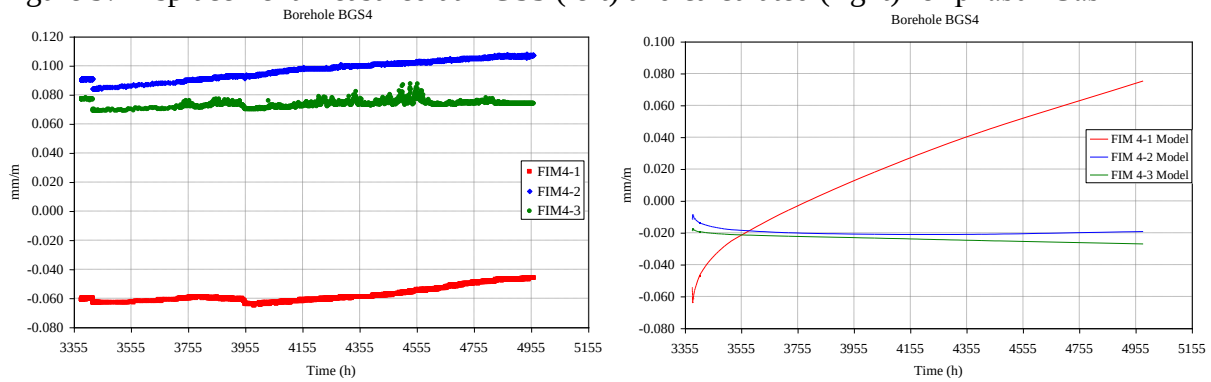

Figure 10: Displacement measured at BGS4 (left) and calculated (right) for phase "Gas2"

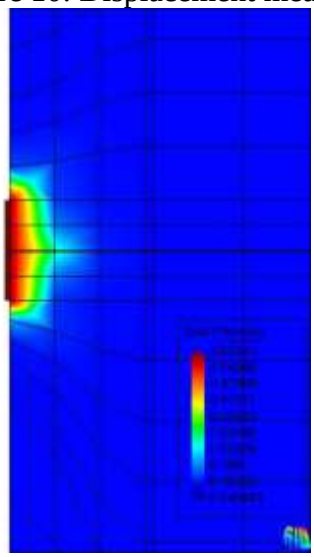

Figure 11: Contour plot of gas pressure at time 4964 hours

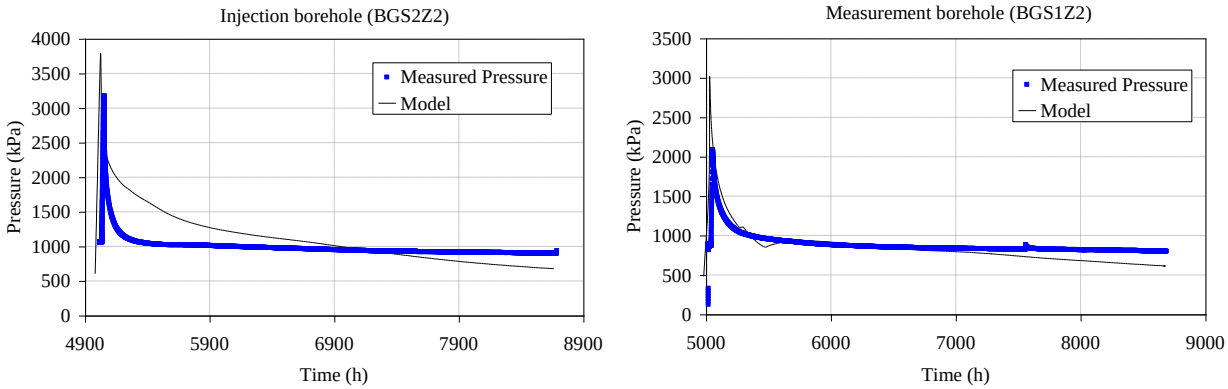

Figure 12: Comparison between numerical and experimental pressures at injection borehole BGS2 and at measurement borehole BGS1 for phase "Gas 3"

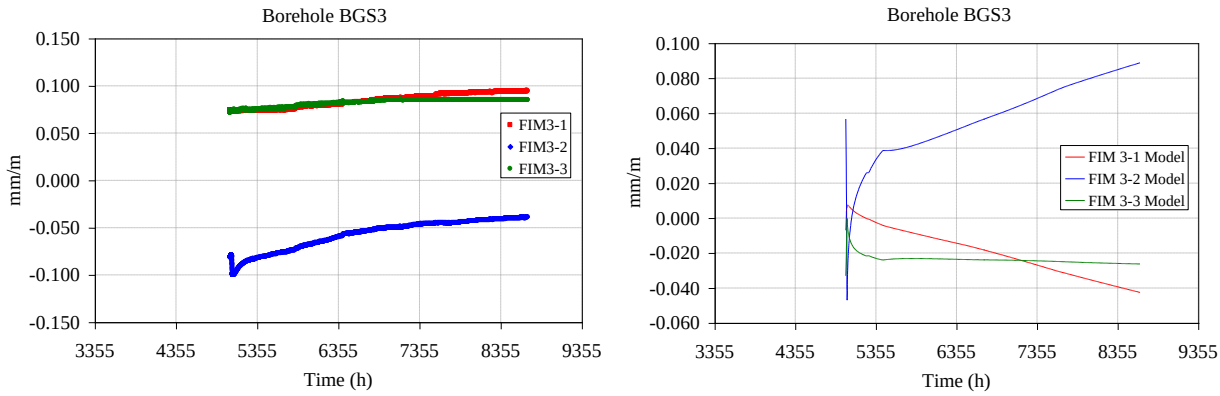

Figure 13: Displacement measured at BGS3 (left) and calculated (right) for phase “Gas 3”

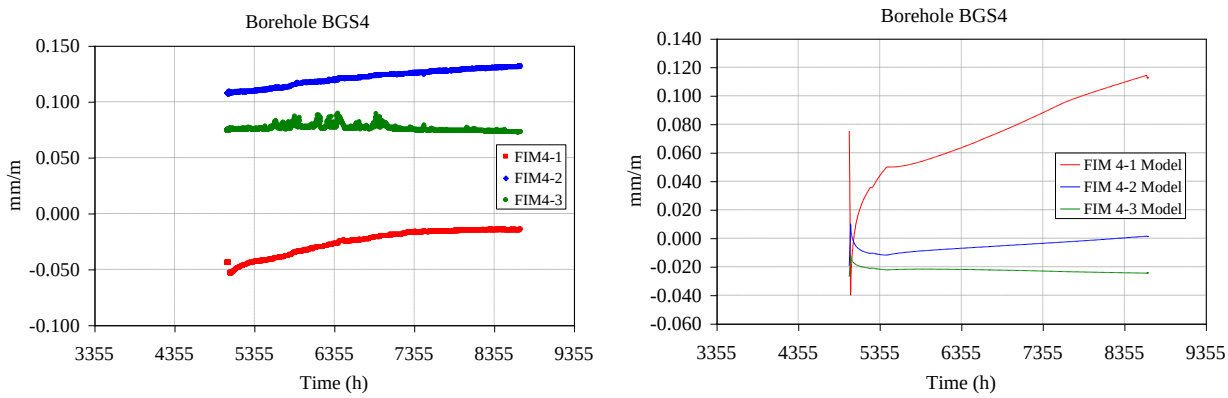

Figure 14: Displacement measured at BGS4 (left) and calculated (right) for phase “Gas 3”

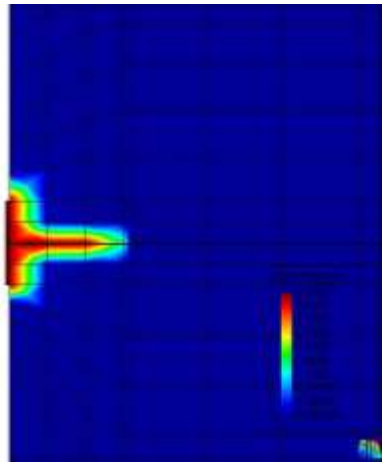

Figure 15: Contour plot of gas pressure at time 5029 hours

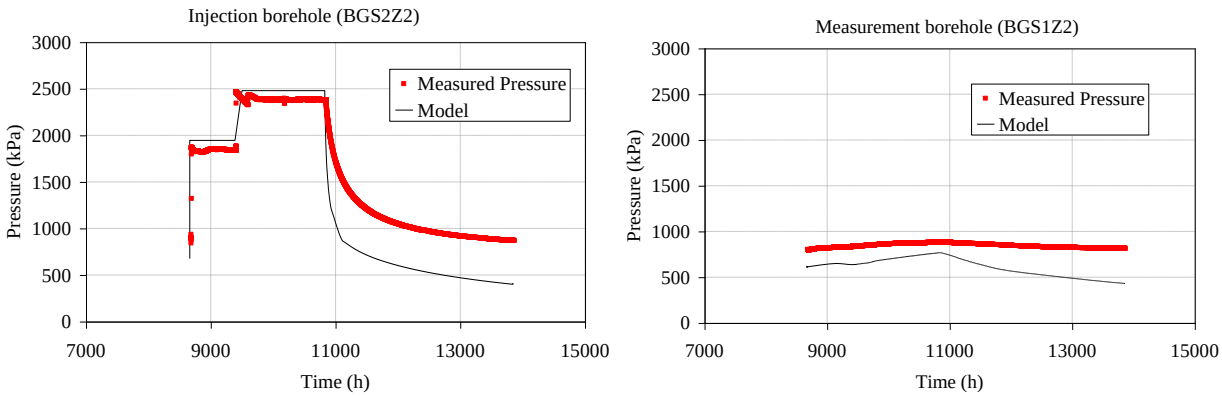

Figure 16: Comparison between numerical and experimental pressures at injection borehole BGS2 and at measurement borehole BGS1 for phase “Hydro 3”

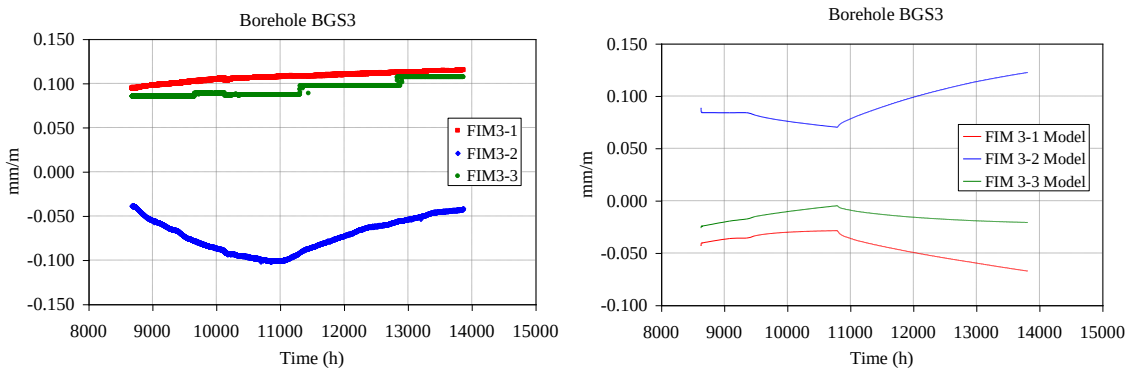

Figure 17: Displacement measured at BGS3 (left) and calculated (right) for phase “Hydro 3”

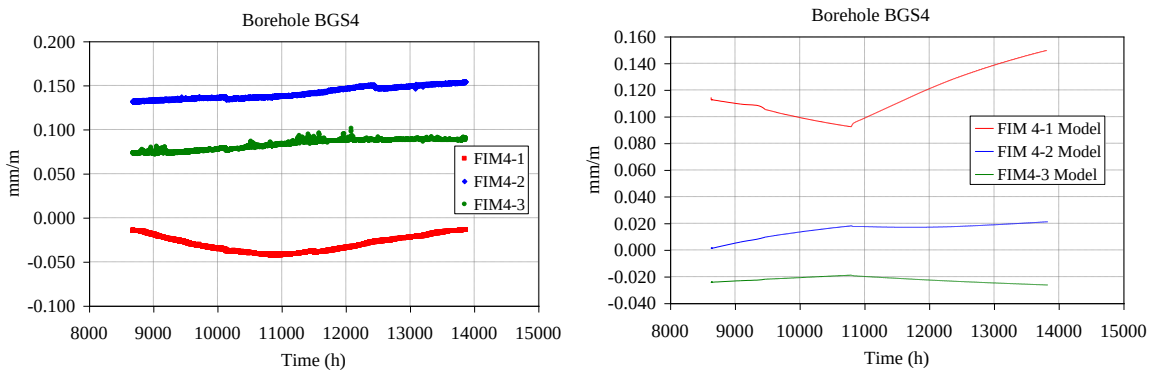

Figure 18: Displacement measured at BGS4 (left) and calculated (right) for phase “Hydro 3”

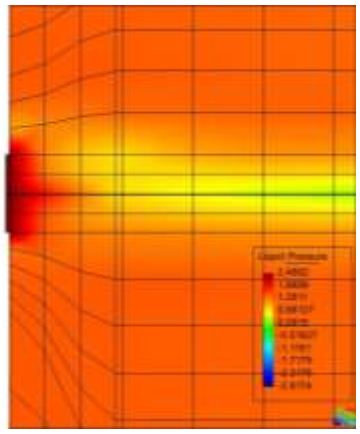

Figure 19: Contour plot of liquid pressure at time 10826 hours

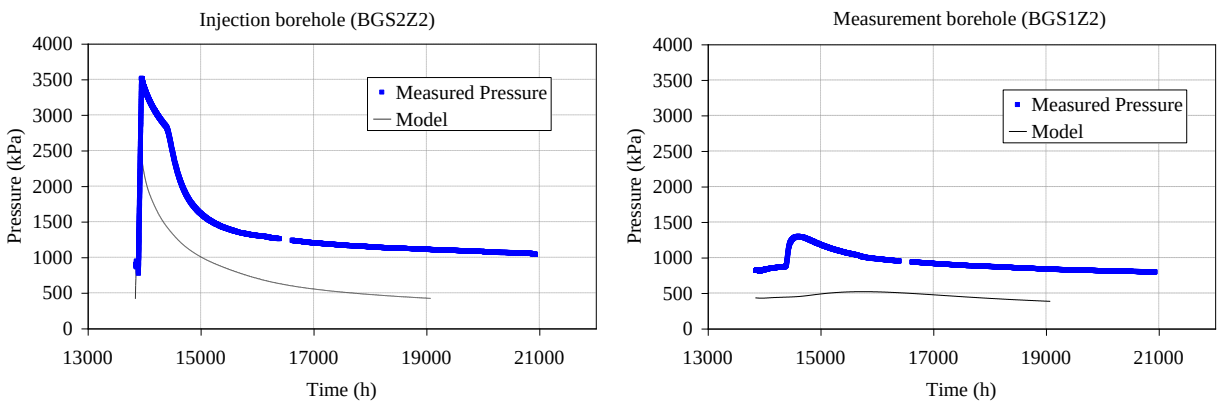

Figure 20: Comparison between numerical and experimental pressures at injection borehole BGS2 and at measurement borehole BGS1 for phase “Gas 4”

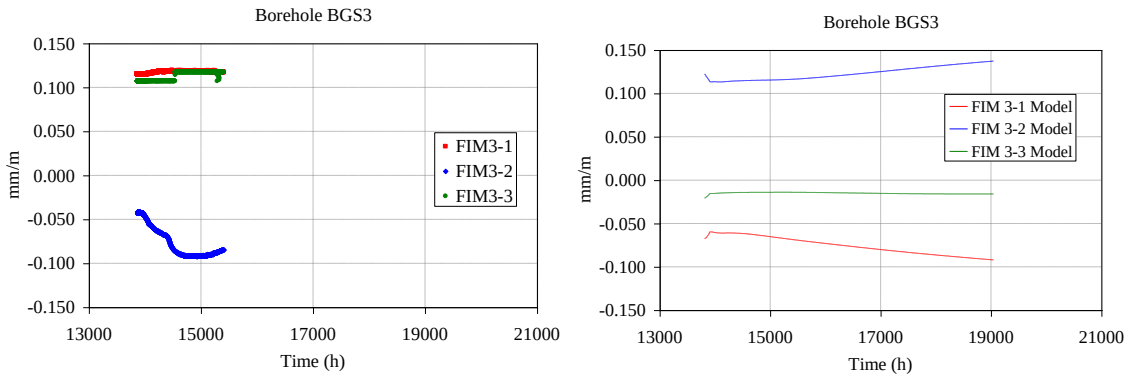

Figure 21: Displacement measured at BGS3 (left) and calculated (right) for phase “Gas 4”

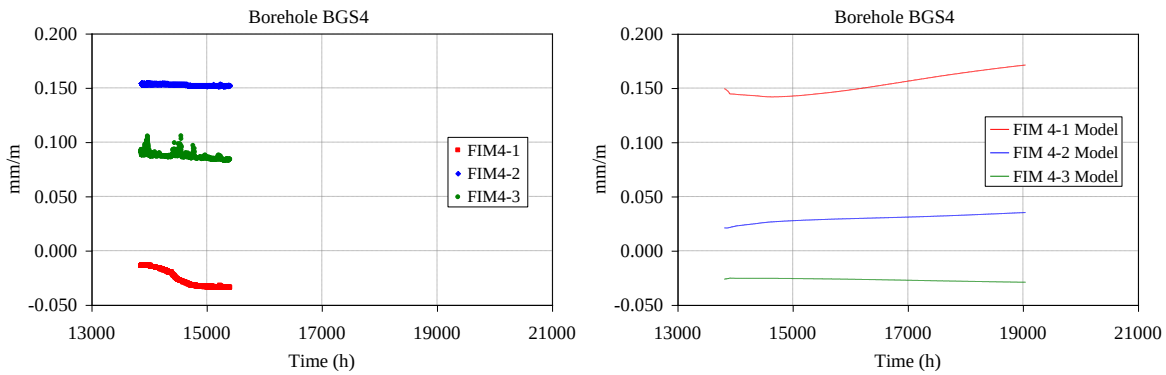

Figure 22: Displacement measured at BGS4 (left) and calculated (right) for phase “Gas 4”

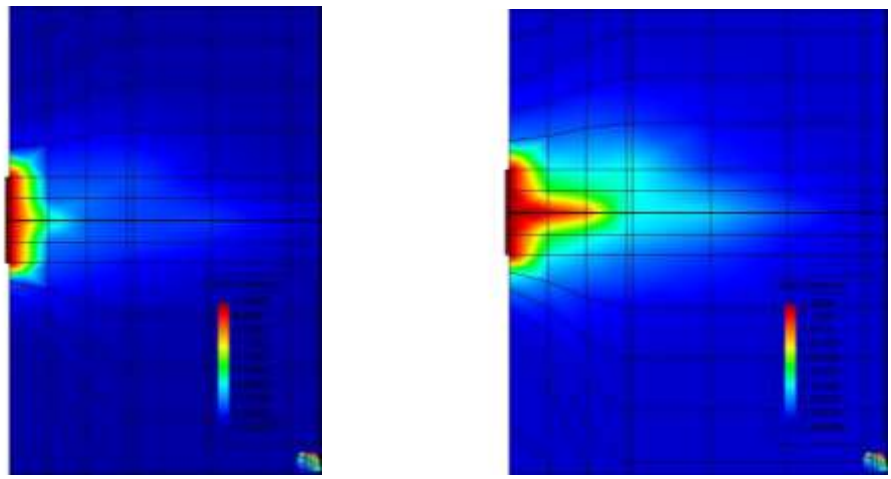

Figure 23: Contour plot of gas pressure at time 13936 hours (left) and at time 14611hours (right)

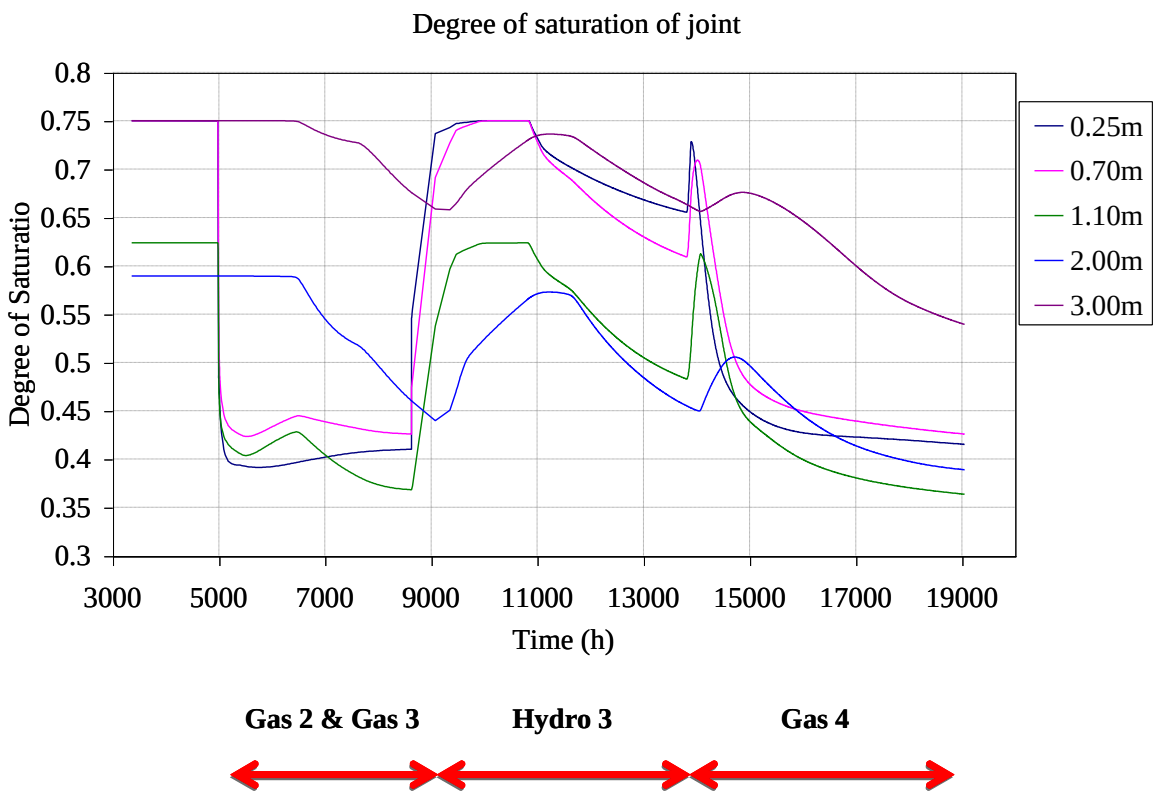

Figure 24: Degree of saturation of the Fracture at different distance from the injection borehole

Conclusions

From the comparison of the test results it is possible conclude that the evolution of pressure are well captured by the model. However, a refine comparison of the displacements would be necessary.

It is recommended confirm the gas flow rate at phase Gas 2.

Also, the variation of the permeability and compressibility of the Fracture should be analyzed during the test.

References

Barton N., Bandis S. & Bakhtar K. (1985), *Strength, deformation and conductivity coupling of rock joints*. Int. Journal of Rock Mechanics and Mining Science & Geomechanics Abst, 22(3):121–140

Enachescu C., Blüming, P., Castelao, A. & Steffen P. (2002) Mont-Terri GP-A and GS Experiments Synthesis Report, Interner Bericht 02-51.

Olivella, S. & Alonso, E. E. (2008). Gas flow through clay barrier. Geotechnique 58 No. 3, 157–176.

Sánchez, M. (2004), Thermo-hydro- mechanical coupled analysis in low permeability media. Ph.D. Thesis. Universitat Politècnica de Catalunya (UPC). 281 pp. Barcelona.

Van Genuchten, M. Th. (1980). A closed-form equation for predicting the hydraulic conductivity of unsaturated soils. Soil Sci. Soc.Am. J. 49, No. 9, 892–898